

SUPPLEMENTARY DATA

**Supplementary Table 1.** Specification of the 11 $\beta$ -HSD1 inhibitor UE2316

**11 $\beta$ -HSD1 Inhibition data**

Species	IC <sub>50</sub> (nM)*
Human	42
Mouse	126
Rat	80
Monkey	72

\*IC<sub>50</sub> data were determined in assays of HEK293 cells stably transfected with the full length HSD11B1 genes for each species.

\*Sooy K, Webster SP, Noble J, Binnie M, Walker BR, Seckl JR, Yau JL. Partial deficiency or short-term inhibition of 11 $\beta$ -hydroxysteroid dehydrogenase type 1 improves cognitive function in aging mice. *J. Neurosci.* 2010;**30**:13867-13872.

**Supplementary Table 2.** Differentially expressed genes determined by microarray in islets from high fat fed MIP-HSD1<sup>tg/+</sup> versus KsJ mice. Isolated islets from 12 weeks high fat-fed KsJ and MIP-HSD1<sup>tg/+</sup> mice were analysed using Affymetrix mouse genechip 2.0 (n=4 replicates from islets pooled from 2 to 3 mice per replicate). Genes with a fold-change over 1.5 and statistically significant difference from control mice (versus KsJ HF, *P*<0.05) were analysed and sorted into functional groups using the David bioinformatics resource 6.7 software. The 5 most enriched functional clusters are listed.

Function	EntrezGene ID	Name		Fold Change	Raw P value
<b>Stress Response</b>					
	15511	heat shock protein 1B	Hspa1b	2.21	0.024
	193740	heat shock protein 1A	Hspa1a	2.11	0.038
	15525	heat shock protein 4	Hspa4	1.66	0.010
	15505	heat shock 105kDa/110kDa protein 1	Hsph1	1.64	0.032
	15519	heat shock protein 90, alpha (cytosolic), class A member 1	Hsp90aa1	1.55	0.003
	56295	HIG1 domain family, member 1A	Higd1a	-1.58	0.0001
	12696	cold inducible RNA binding protein	Cirbp	-1.6	0.048
<b>Gene transcription</b>					
	29808	MAX gene associated	Mga	1.8	0.005
	79221	histone deacetylase 9	Hdac9	1.75	0.007
	228775	tribbles homolog 3 (Drosophila)	Trib3	1.74	0.007
	18789	poly (A) polymerase alpha	Papola	1.74	0.011
	19345	RAB5C, member RAS oncogene family	Rab5c	1.73	0.020

SUPPLEMENTARY DATA

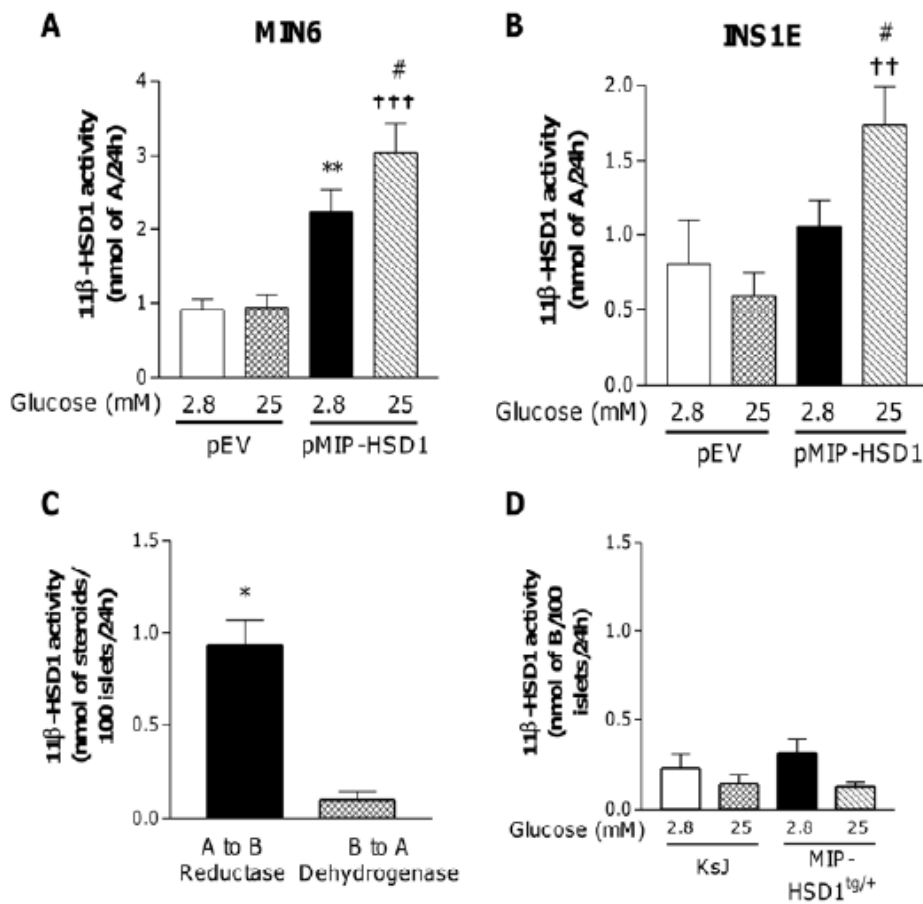
	270110	interferon regulatory factor 2 binding protein 2	Irf2bp2	1.62	0.024
	100048299/ 17187	similar to Myn protein / Max protein	LOC10004 8299 /// Max	1.56	0.011
	63856	TAF8 RNA polymerase II, TATA box binding protein (TBP)-associated factorq	Taf8	1.53	0.018
	19330	RAB18, member RAS oncogene family	Rab18	-1.56	0.009
<b>Signal transduction</b>					
Small GTPase pathway	19734	regulator of G-protein signaling 16	Rgs16	2.73	0.002
	18749	protein kinase, cAMP dependent, catalytic, beta	Prkacb	2.19	0.009
	19345	RAB5C, member RAS oncogene family	Rab5c	1.73	0.020
	14579	GTP binding protein (gene overexpressed in skeletal muscle)	Gem	1.68	0.000
	11845	ADP-ribosylation factor 6	Arf6	1.65	0.014
	75547	A kinase (PRKA) anchor protein 13	Akap13	1.63	0.008
	79264	KRIT1, ankyrin repeat containing	Krit1	1.53	0.004
	11841	ADP-ribosylation factor 2	Arf2	-1.54	0.002
	19330	RAB18, member RAS oncogene family	Rab18	-1.56	0.009
MAPK pathway	15511	heat shock protein 1B	Hspa1b	2.21	0.024
	18749	protein kinase, cAMP dependent, catalytic, beta	Prkacb	2.19	0.009
	29808	MAX gene associated	Mga	1.8	0.005
	109880	Braf transforming gene	Braf	1.72	0.016
	100048299/ 17187	similar to Myn protein / Max protein	LOC10004 8299 /// Max	1.56	0.011
	17762	microtubule-associated protein tau	Mapt	1.51	0.0002
Jak-Stat pathway	12444	cyclin D2	Ccnd2	1.62	0.009
	16451	Janus kinase 1	Jak1	1.56	0.018
	12700	cytokine inducible SH2-containing protein	Cish	1.52	0.005
	12702	suppressor of cytokine signaling 3	Socs3	1.51	0.042
<b>Vesicle transport</b>					
	56491	vesicle-associated membrane protein, associated protein B	Vapb	1.81	0.008

SUPPLEMENTARY DATA

		and C			
	11845	ADP-ribosylation factor 6	Arf6	1.65	0.014
	68137	KDEL (Lys-Asp-Glu-Leu) endoplasmic reticulum protein retention receptor 1	Kdelr1	1.63	0.011
	12890	complexin 2	Cplx2	1.63	0.031
	71770	adaptor-related protein complex 2, beta 1 subunit	Ap2b1	1.62	0.032
	17775	lysosomal-associated protein transmembrane 4A	Laptm4a	1.59	0.016
	74732	syntaxin 11	Stx11	1.56	0.021
	70361	lectin, mannose-binding, 1	Lman1	1.5	0.009
	11841	ADP-ribosylation factor 2	Arf2	-1.54	0.002
	27096	trafficking protein particle complex 3	Trappc3	-1.61	0.0004
	18111	neuronatin	Nnat	-1.65	0.004
<b>Proliferation/ cell growth</b>					
	12575	cyclin-dependent kinase inhibitor 1A (P21)	Cdkn1a	1.63	0.006
	21825 / 64044	similar to thrombospondin 1/ thrombospondin 1	LOC64044 1 /// Thbs1	1.63	0.0003
	12444	cyclin D2	Cend2	1.62	0.009
	19156	prosaposin	Psap	1.61	0.023
	16451	Janus kinase 1	Jak1	1.56	0.018
	63856	TAF8 RNA polymerase II, TATA box binding protein (TBP)-associated factorq	Taf8	1.53	0.018
	13193	doublecortin	Dcx	1.53	0.0002
	19684	radixin	Rdx	1.52	0.021
	12700	cytokine inducible SH2-containing protein	Cish	1.52	0.005
	17762	microtubule-associated protein tau	Mapt	1.51	0.0002
	12702	suppressor of cytokine signaling 3	Socs3	1.51	0.042
	13616	endothelin 3	Edn3	-1.56	0.002

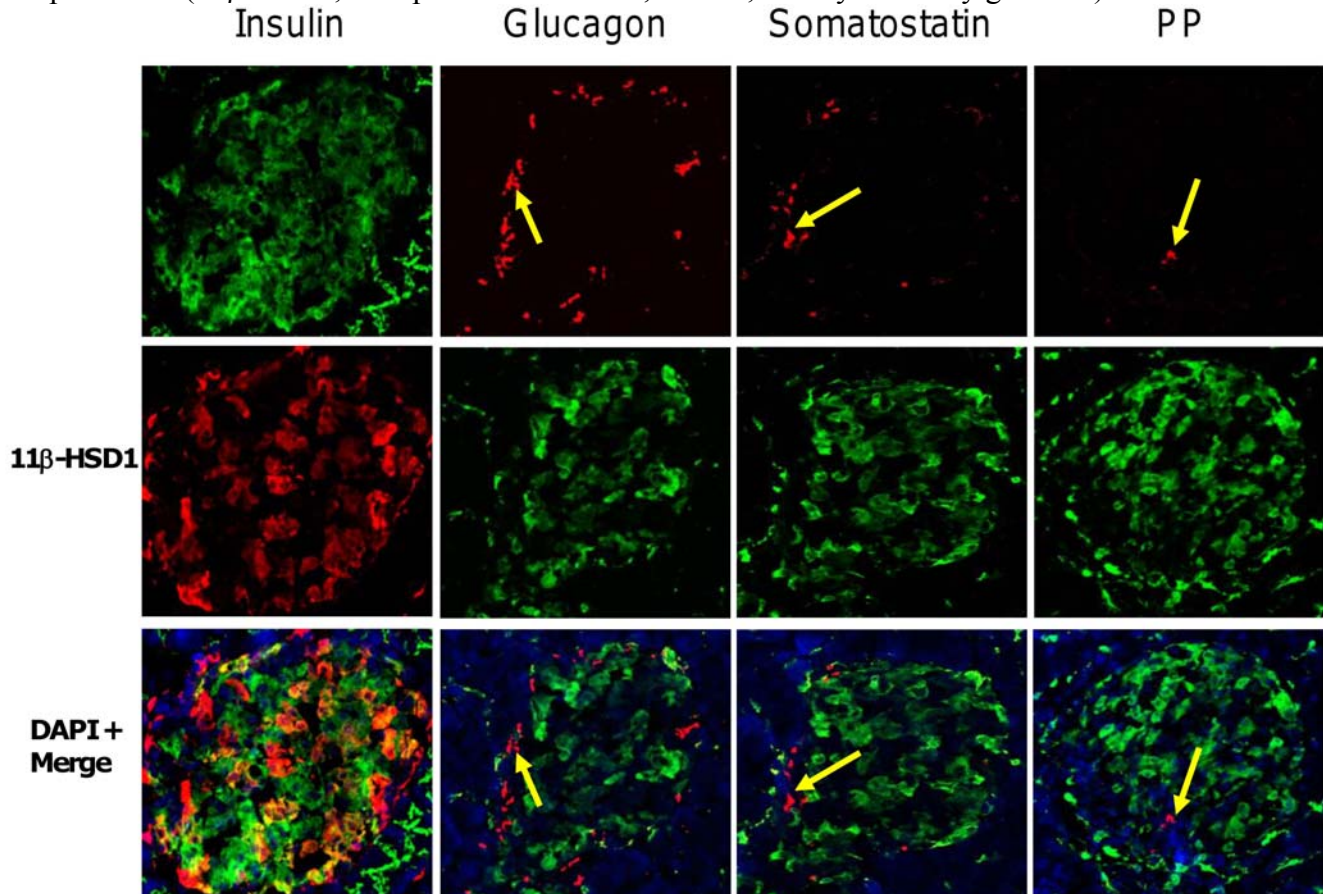
SUPPLEMENTARY DATA

**Supplementary Figure 1.**  $11\beta$ -HSD1 activity in  $\beta$ -cell cell lines and isolated islets. (A) MIN6 or (B) INS1E  $\beta$ -cell cell lines were transfected with either empty vector (pEV- white and hatched bars) or plasmid containing the MIP-HSD1 transgene (pMIP-HSD1, black and diagonally striped bars).  $11\beta$ -HSD1 activity was assayed with low (2.8 mmol/l-white and black bars) or high (25 mmol/l- hatched and diagonally striped bars) glucose concentrations in the presence of 210 nmol/l  $11$ -DHC for 24 h. \*\* =  $P < 0.01$  pMIP-HSD1 2.8 vs pEV 2.8,  $\bullet\bullet\bullet = P < 0.001$  pMIP-HSD1 25 vs pEV 25, # =  $P < 0.05$  pMIP-HSD1 25 vs pMIP-HSD1 2.8,  $\bullet\bullet = P < 0.01$  pMIP-HSD1 25 vs pEV 25, n=6 done in triplicates. (C)  $11\beta$ -HSD1 activity assayed in 100 isolated islets of KsJ mice treated for 24 h in presence of either  $11$ -DHC (A) (black bar) or corticosterone (B) (hatched bar) and expressed in nanomols of B or A metabolised respectively, \* =  $P < 0.05$  n= 5. (D) Dehydrogenase activity assayed in 100 isolated islets of KsJ (white and hatched bars) and MIP-HSD1<sup>tg/+</sup> (black and diagonally striped bars) mice treated 24 h with corticosterone (B) in 2.8 mmol/l (white and black bars) or 25 mmol/l (hatched and diagonally striped bars) glucose and expressed in nanomols of B metabolised into A (n= 4).



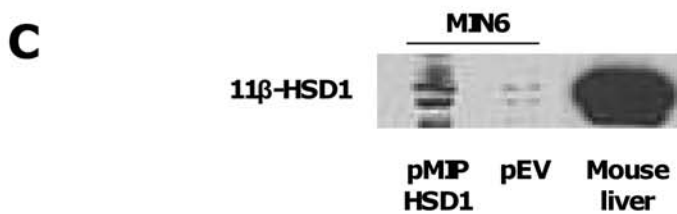
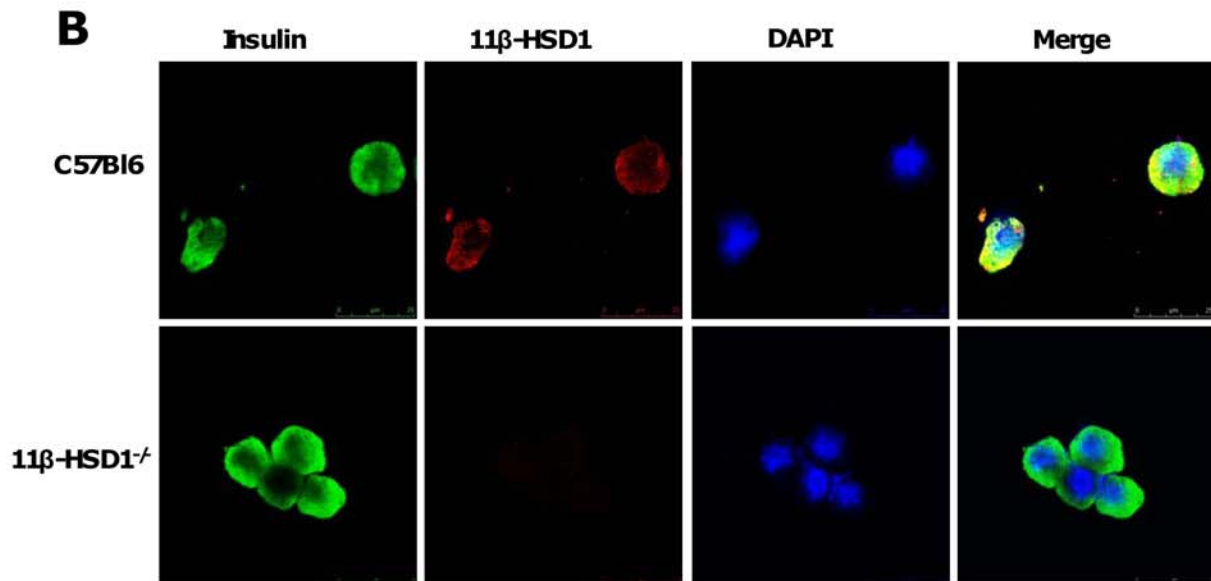
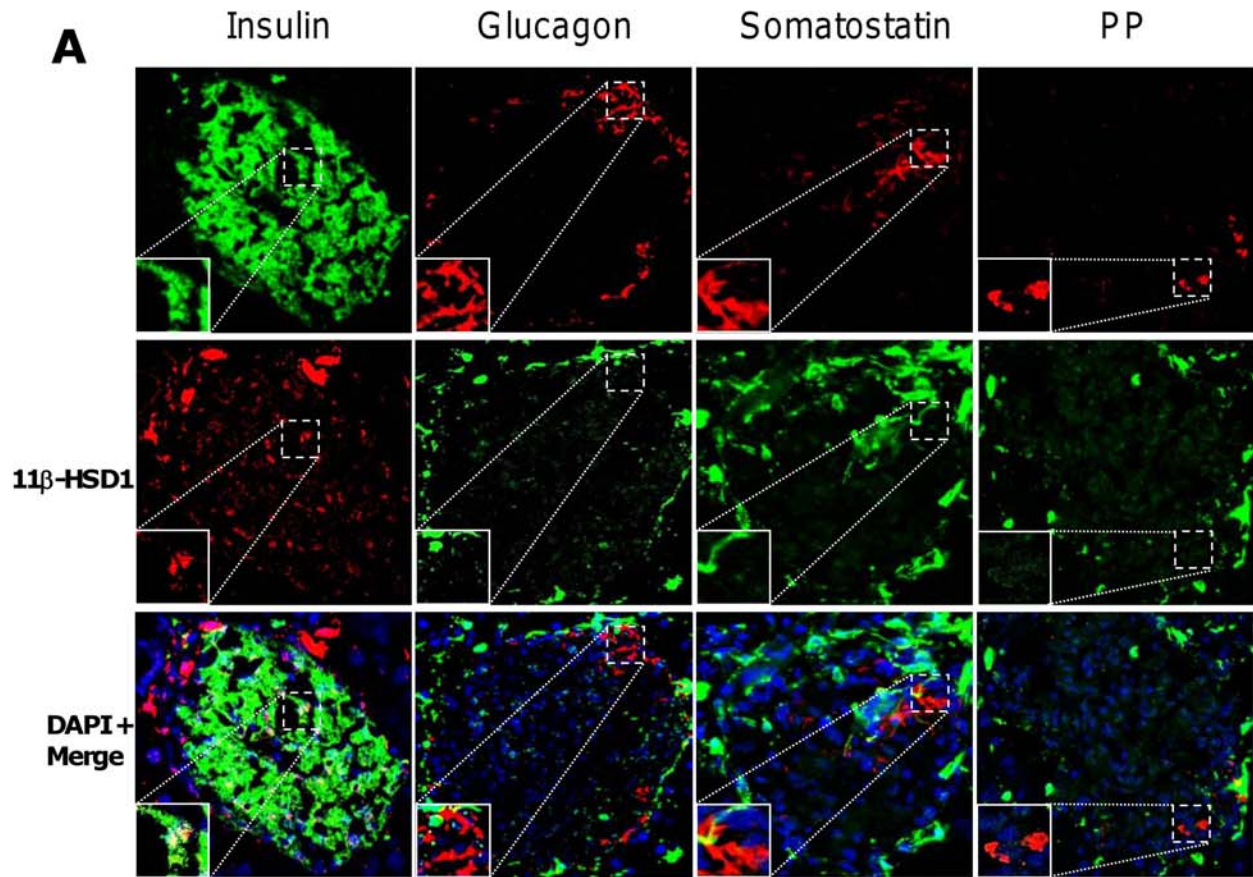
SUPPLEMENTARY DATA

**Supplementary Figure 2.** Transgene mediated overexpression of 11 $\beta$ -HSD1 colocalises with insulin in MIP-HSD1<sup>tg/+</sup> mice islets. Representative confocal immunofluorescent microscopy on frozen pancreata sections from MIP-HSD1<sup>tg/+</sup> mice stained for 11 $\beta$ -HSD1 (middle row) and either insulin, glucagon, somatostatin or pancreatic polypeptide (PP) (upper row). The merged pictures (bottom row) are supplemented with nuclear DAPI staining in blue. Magnification x40. The yellow arrows highlight cell-specific staining of either glucagon ( $\alpha$  cells), somatostatin ( $\delta$  cells) or PP (pp cells). Note that 11 $\beta$ -HSD1 and insulin appear partially co-localised due to their predominant distribution in different subcellular compartments (11 $\beta$ -HSD1; endoplasmic reticulum, insulin; mainly secretory granules).



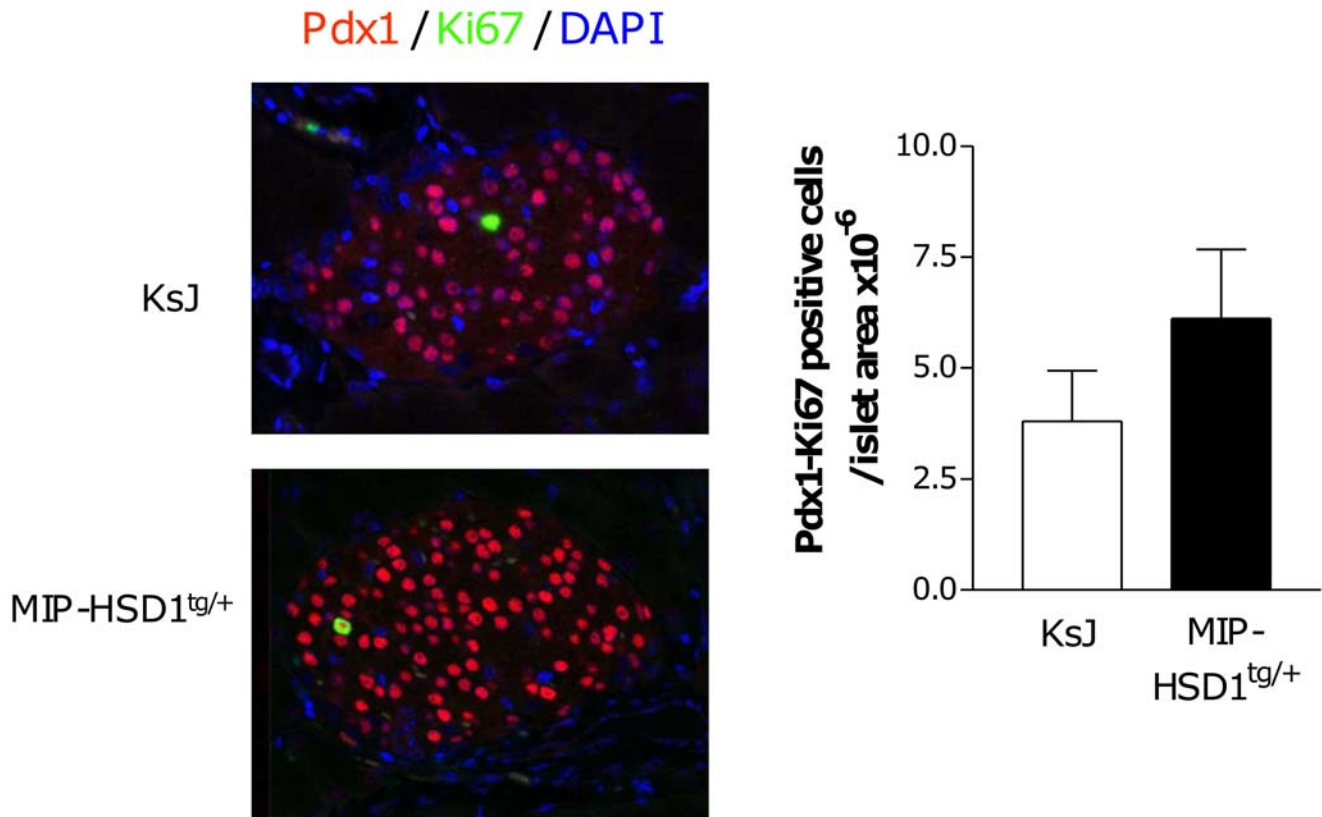
**Supplementary Figure 3.** 11 $\beta$ -HSD1 colocalises with insulin-positive  $\beta$ -cells in KsJ (normal) islets. (A). Representative confocal immunofluorescent microscopy on frozen pancreata sections from KsJ mice stained for 11 $\beta$ -HSD1 (middle row) and either insulin, glucagon, somatostatin or pancreatic polypeptide (PP) (upper row). Merged pictures (bottom row) show additional nuclear DAPI staining in blue. Magnification x40. Each inset square window represents x2 magnification of the chosen area (dashed lines) highlighting co-localisation of 11 $\beta$ -HSD1 with cell-specific staining of insulin ( $\beta$ -cell), glucagon ( $\alpha$  cells), somatostatin ( $\delta$  cells) or PP (pp cells). Note that the insulin merge indicates extensive co-localisation with insulin positive cells but that 11 $\beta$ -HSD1 (endoplasmic reticulum) has a distinct subcellular distribution to insulin (mainly secretory granules) and thus a lower than expected ‘yellow’ merge colour expression pattern is obtained. (B). Representative immunofluorescent images of trypsin-digested single islet cells showing co-staining for insulin and 11 $\beta$ -HSD1 (upper panels) in C57BL/6J but not 11 $\beta$ -HSD1<sup>-/-</sup> mice. (C). Western blot of 11 $\beta$ -HSD1 in lysates of clonal MIN6  $\beta$ -cells transfected (leftmost lane) with the MIP-HSD1 construct, an empty vector (basal 11 $\beta$ -HSD1; middle lane) and in mouse liver lysates (rightmost lane).

SUPPLEMENTARY DATA



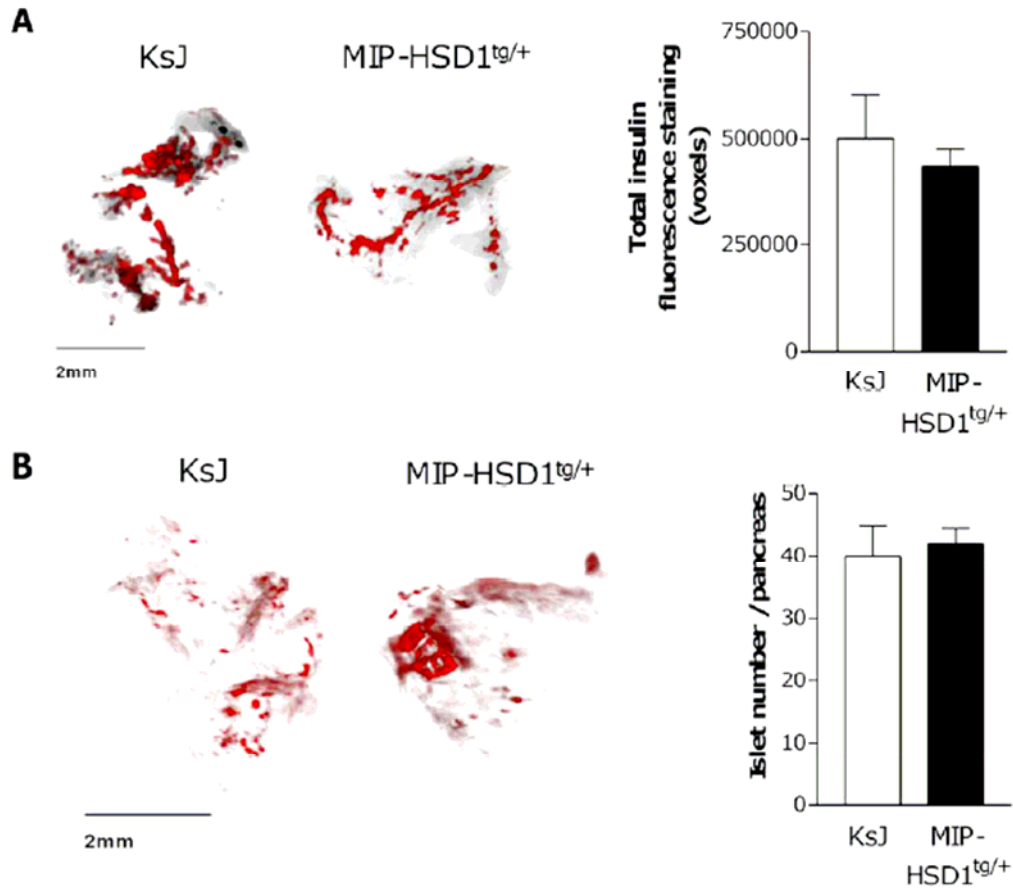
SUPPLEMENTARY DATA

**Supplementary Figure 4.** Comparable  $\beta$ -cell replication in adult KsJ and MIP-HSD1<sup>tg/+</sup> islets. Representative confocal immunofluorescent microscopy on paraformaldehyde fixed paraffin embedded pancreata sections from KsJ and MIP-HSD1<sup>tg/+</sup> mice stained for Pdx1 (red), Ki67 (green) and DAPI (in blue) with quantification of double positive Pdx1/Ki67 cells per islet area (ns, n=4-6 mice, 5-13 images). Magnification x40.



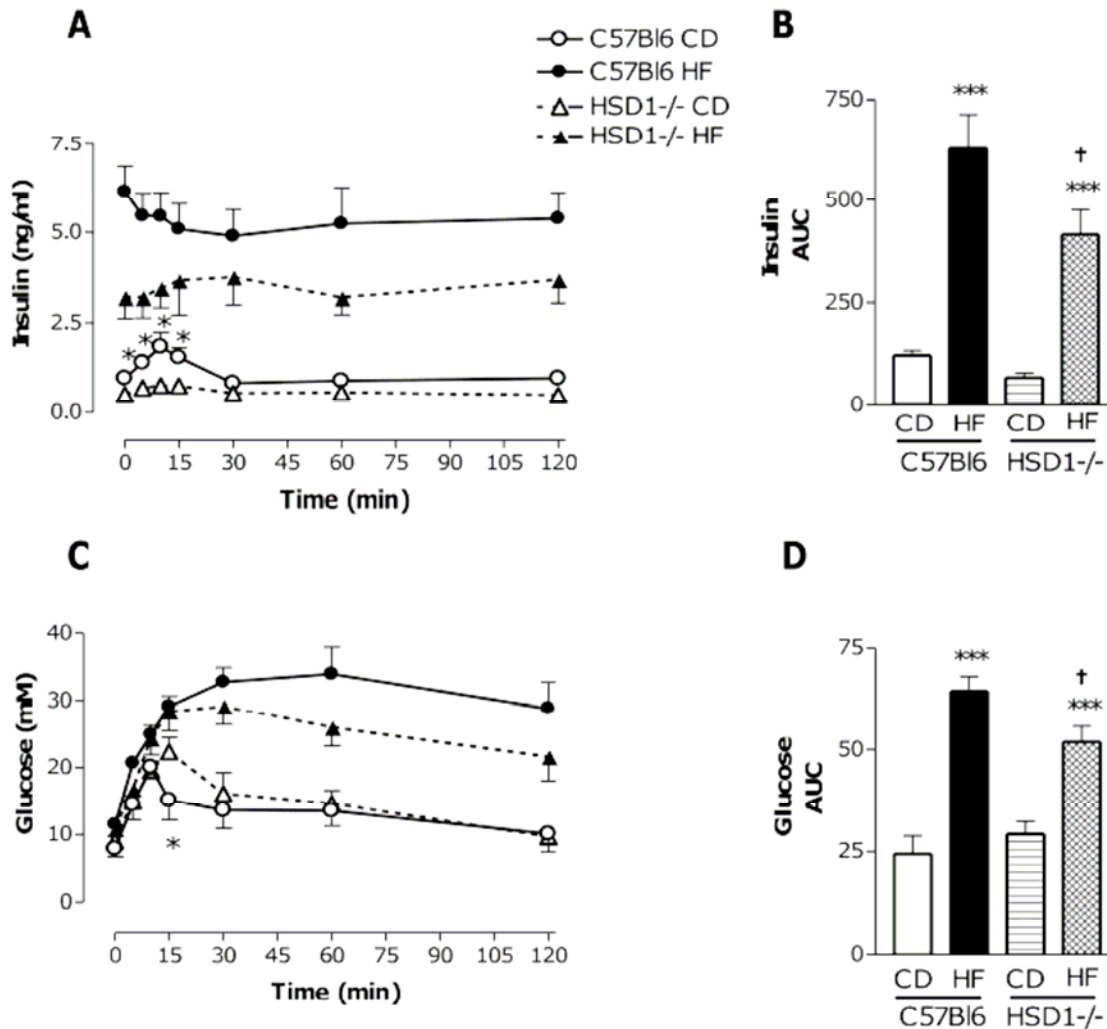
SUPPLEMENTARY DATA

**Supplementary Figure 5.** Equivalent insulin content between KsJ and MIP-HSD1<sup>tg/+</sup> pancreata at stage E18 and newborn. OPT images of (A) embryonic stage E18 and (B) newborn pancreata from KsJ and MIP-HSD1<sup>tg/+</sup> mice immunostained for insulin. Quantification of total fluorescence emitted (A) or insulin positive islets (B) per specimen is represented in bar graphs adjacent to the pictures (n=4).



SUPPLEMENTARY DATA

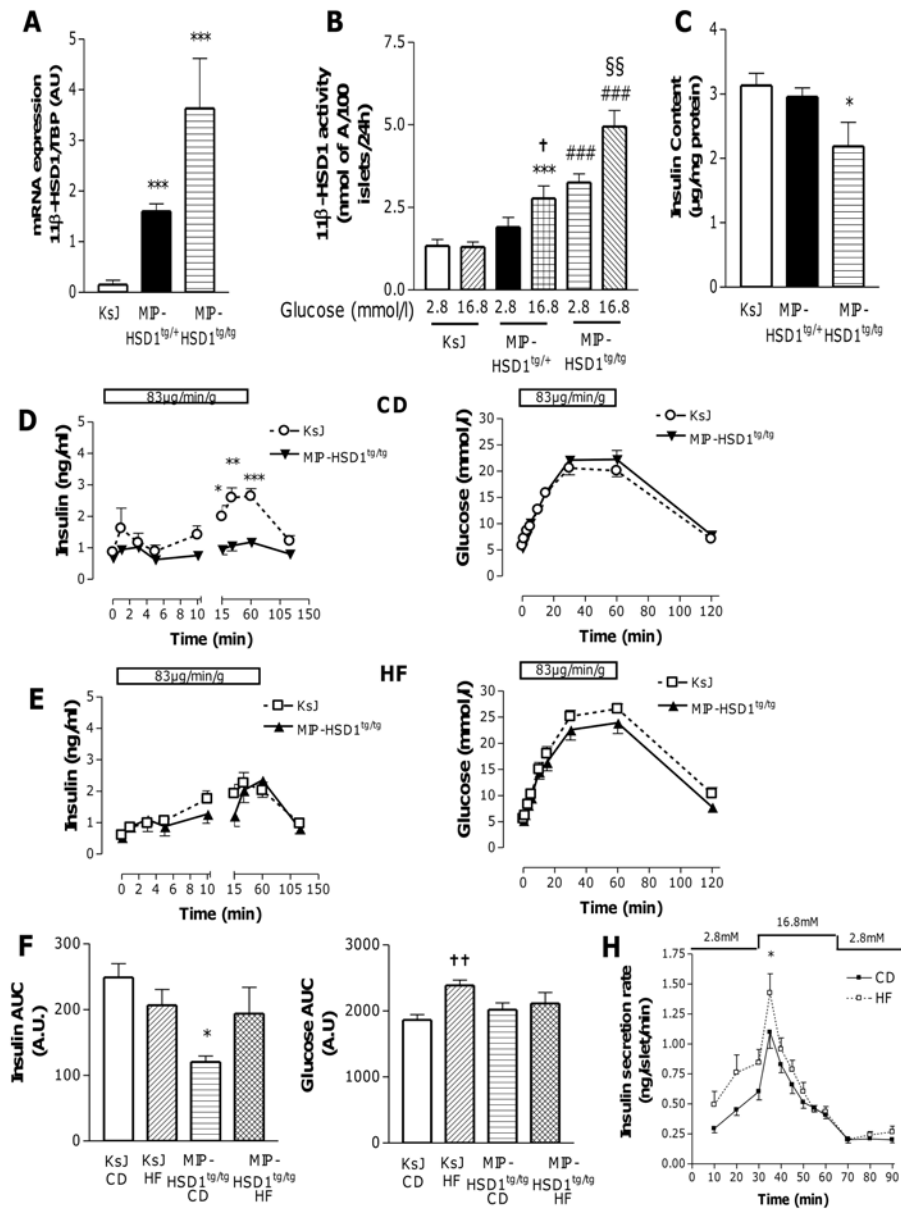
**Supplementary Figure 6.**  $11\beta$ -HSD1<sup>-/-</sup> mice have a mild secretory defect offset by peripheral insulin sensitisation. Dynamic (A) and A.U.C (B) insulin and dynamic (C) and (D) A.U.C. glucose levels during a glucose tolerance test in C57BL/6 (circle symbols, solid lines) and  $11\beta$ -HSD1<sup>-/-</sup> (triangle symbols, broken lines) mice after 18 weeks on control (CD, open symbols; white and horizontal stripes bars) or high fat diet (HF, solid symbols, black and diagonally cross-hatched bars). \* =  $P < 0.05$  for C57BL/6 CD vs  $11\beta$ -HSD1<sup>-/-</sup> CD, n=6. A.U.C for (B) insulin and (D) glucose level; \*\*\* =  $P < 0.001$  for HF vs CD for both genotypes, n=6; † =  $P < 0.05$  for  $11\beta$ -HSD1<sup>-/-</sup> HF vs C57BL/6 HF, n=6.



## SUPPLEMENTARY DATA

**Supplementary Figure 7.** Homozygous MIP-HSD1tg/tg mice exhibit a partially impaired b-cell secretory phenotype. (A) 11b-HSD1 mRNA level measured by real time PCR in isolated islets of KsJ (white bar), MIP-HSD1tg/+ (black bar) and MIP-HSD1tg/tg (horizontally striped bar) mice and normalised to TBP gene expression. \*\*\* = $P < 0.001$  for MIP-HSD1tg/tg and MIP-HSD1tg/+ vs KsJ  $n=5$  in triplicates. (B) 11b-HSD1 activity in isolated islets of KsJ (white and left diagonally striped bars), MIP-HSD1tg/+ (black and square hatched bars) and MIP-HSD1tg/tg (horizontally and right diagonally striped bars) mice treated for 24 h with 2.8 mmol/l (white, black and horizontally striped bars) or 16.8 mmol/l (left diagonally, square-hatched and right diagonally stripes bars) glucose concentrations in presence of 210nM of 11DHC. \*\*\* = $P < 0.001$  for MIP-HSD1tg/+ 16.8 vs KsJ 16.8; ... = $P < 0.05$  for MIP-HSD1tg/+ 16.8 vs MIP-HSD1tg/+ 2.8, ### = $P < 0.001$  for MIP-HSD1tg/tg 2.8 vs KsJ 2.8 and MIP-HSD1tg/tg 16.8 vs KsJ 16.8; §§ = $P < 0.01$  for MIP-HSD1tg/tg 16.8 vs MIP-HSD1tg/tg 2.8. (C) Whole pancreas insulin content over total protein content of KsJ (white bar), MIP-HSD1tg/+ (black bar) and MIP-HSD1tg/tg (horizontally striped bar) mice measured by RIA (\* = $P < 0.05$ ,  $n=6$ ). After 12 weeks of either (D) control (CD) or (E) high fat (HF) diet MIP-HSD1tg/tg mice (black triangles-solid line) were infused with glucose (83 $\mu$ g/min/g for 1h) through a jugular cannula as in Fig. 2. Insulin (left panel) and glucose (right panel) were measured at the indicated time points and compared with KsJ control mice (white circles and squares - dotted line) reported from Fig. 2.. \* = $P < 0.05$ , \*\* = $P < 0.01$ , \*\*\* = $P < 0.001$  MIP-HSD1tg/tg CD vs KsJ CD  $n=7$ . (F) Area under the curves for insulin (left panel) and glucose (right panel) levels between KsJ (reported from Fig. 2- white and diagonally striped bars) and MIP-HSD1tg/tg (vertically striped and hatched bars) mice under in vivo glucose infusion. \* = $P < 0.05$  for MIP-HSD1tg/tg CD vs KsJ CD, ..... = $P < 0.01$  for KsJ HF vs KsJ CD,  $n=7$ . (G) Insulin secretion rate was measured in batches of 10 size-matched isolated islets from MIP-HSD1tg/tg mice on control (CD-black squares-solid line) or high fat diet (HF-white squares-dotted line) with either 2.8 mmol/l or 16.8 mmol/l glucose. \* = $P < 0.05$ ,  $n=6$ , in triplicates.

SUPPLEMENTARY DATA



SUPPLEMENTARY DATA

**Supplementary Figure 8.** 11 $\beta$ -HSD1 is permissive for palmitate-induced GSIS in isolated islets from 11 $\beta$ -HSD1<sup>tg/+</sup> mice. Isolated islets from MIP-HSD1<sup>tg/+</sup> mice on control diet were treated 24h with 20 nmol/l 11-DHC only (black bar) or supplemented with 0.5 mmol/l palmitate (white bar) in the presence or absence of the selective 11 $\beta$ -HSD1 inhibitor UE2316 (vertically striped bar) or GR inhibitor RU486 (horizontally striped bar). \* =*P*<0.05 for palmitate vs none, †=*P*<0.05 for UE2316 vs palmitate, # =*P*<0.05 for RU486 vs palmitate, n=4-8

